

$O(g)$ plasma effects in jet quenching

Simon Caron-Huot*

Physics Department, McGill University, 3600 rue University, Montréal, QC H3A 2T8, Canada

(Received 22 January 2009; published 31 March 2009)

We consider the bremsstrahlung energy loss of high-energy partons moving in the quark-gluon plasma, at weak coupling. We show that the rates for these processes receive large $O(g)$ corrections from classical (non-Abelian) plasma physics effects, which are calculated. In the high-energy (deep Landau-Pomeranchuk-Migdal) regime these corrections can be absorbed in a change of the transverse momentum broadening coefficient \hat{q} , which we give to the next-to-leading order. The correction is large even at relatively weak couplings $\alpha_s \sim 0.1$, as is typically found for such effects, signaling difficulties with the perturbative expansion. Our approach is based on an effective Euclideanization property of classical physics near the light cone, which allows an effective theory approach in Euclidean space and suggests new possibilities for the nonperturbative lattice study of these effects.

DOI: 10.1103/PhysRevD.79.065039

PACS numbers: 11.10.Wx, 12.38.Mh

I. INTRODUCTION

The phenomenon of jet quenching, or suppression of high- p_T hadrons in $A + A$ collisions relative to expectations from scaling of binary $p + p$ collisions, has been the focus of much recent interest at the Relativistic Heavy Ion Collider (RHIC) [1,2]. Its theoretical description (see, e.g., [3] and references therein) is based on the theory of jet evolution in thermalized media, whose uncertainties it is thus worthwhile to seek to reduce, or at least, quantify. This requires the calculation of higher-order effects, which we propose to do in this paper in the regime of weak coupling.

As established by a large body of work on the thermodynamic pressure [4–6], finite temperature perturbation theory meets with serious convergence difficulties. Unless the strong coupling α_s obeys $\alpha_s \lesssim 0.1$, a strict perturbation theory in powers of g may not be reliable. Such a behavior appears to be generic: it is also observed for the next-to-leading order [NLO or $O(g)$] corrections to thermal masses [7–9], as well as for the only transport coefficient presently known at NLO, heavy quark momentum diffusion [10] (whose behavior seems to be even worse).

Following Braaten and Nieto [5], who studied the thermodynamic pressure, these large perturbative corrections can be attributed to purely classical (non-Abelian) plasma effects. They have shown this by first making use of the scale separation $gT \ll 2\pi T$ to integrate out the scale $2\pi T$, leaving out a three-dimensional effective theory (“electric QCD” or EQCD) describing the scale $m_D \sim gT$ as well as more infrared scales. The claim then is that contributions from the scale $2\pi T$, as well as the parameters of the effective theory, enjoy well-behaved perturbative series [5,11]; all large corrections are included in the effective theory. Furthermore, by treating this effective theory non-perturbatively using various resummation schemes [9,12]

or the lattice [13], reasonable convergence can be obtained down to $T \sim 3 - 5T_c$.

It is natural to expect large corrections from gT -scale plasma effects in other quantities as well. Unfortunately, for real-time quantities such as are most transport coefficients and collision rates, a resummation program similar to that available in Euclidean space has yet to be fully developed and applied. This is because the real-time description of plasmas requires the hard thermal loop (HTL) theory [14] [which in essence is classical (non-Abelian) plasma physics [15], also known as the Wong-Yang-Mills system [16]], which is arguably more complicated than its Euclidean counterpart EQCD.

In this paper, we aim to point out progress which can be made for a specific class of “real-time” quantities: those which probe physics near the light cone. This includes the collision kernel $C(q_\perp)$ that is relevant for the evolution of jets in transverse momentum space, whose crucial role in the theory of jet quenching will be reviewed below.

To explain the idea, we observe that the soft contribution to $C(q_\perp)$ (that arising from soft collisions with $q_\perp \sim gT$) is described by soft classical fields that are being probed passively by the high-energy jet passing through them. These soft classical fields are the fields surrounding the plasma particles. We now observe that the field components moving collinearly with the jet are not particularly important—the standard calculation of collision rates [17] [or see Eq. (21) below] reveals that the contributing particles move with generic angles in the plasma frame, with even a suppression for the ones collinear to the jet (due to the reduced center-of-mass energy)—which implies that the result must be insensitive to the precise value of the jet velocity $v \approx 1$. The trick is then to set $v = 1 + \epsilon$ —which, though unphysical, cannot affect the answer—thus making the hard particle’s trajectory *spacelike*. This makes Euclidean techniques directly applicable, thereby dramatically simplifying the calculation. In other words, at the classical level $C(q_\perp)$ is more “thermodynamical” than actually dynamical.

*scaronhuot@physics.mcgill.ca

In this paper, we will thus (analytically) compute the full $\mathcal{O}(g)$ corrections to the transverse collision kernel $C(q_\perp)$, describing the evolution of the transverse momentum of a fast particle. The second moment of that kernel gives the phenomenologically interesting momentum broadening coefficient \hat{q} , which we also compute at NLO.

This paper is organized as follows. In Sec. II, we summarize our results and explain their relevance to jet quenching; in particular, we discuss the relevance of the parameter \hat{q} . In Sec. III, we explain our computational strategy and formalism. Details of the calculation of $C(q_\perp)$ and of its (ultraviolet-regulated) second moment \hat{q} are given in Secs. IV and V, respectively. In Sec. VI, we derive, at NLO, the relation between the collision kernel $C(q_\perp)$ for the momentum broadening problem and that for jet evolution—which turns out to be identical to the leading-order relation—and we discuss certain operator ordering issues which could enter higher-order treatments. Finally, in the appendix we relate our approach to a slight generalization of sum rules previously found by Aurenche, Gelis and Zaraket [18].

Alternative estimates of \hat{q} and of jet evolution, based on gauge-string duality (see, for instance, [19–25]), will not be discussed in this paper.

II. RESULTS

A. Collision kernel

The main result of this paper is a full next-to-leading order [$\mathcal{O}(g)$] (analytic) expression for the differential collision rate $C(q_\perp)$, defined as

$$\frac{d\Gamma}{d^2q_\perp/(2\pi)^2} \equiv C(q_\perp), \quad (1)$$

which describes the evolution of the transverse momentum of a hard particle (with $E \geq T$).

The $\mathcal{O}(g)$ corrections to $C(q_\perp)$, given in Eq. (19), are due to gT -scale physics and only arise for $q_\perp \sim gT \ll T$; they are plotted in Fig. 1. Both the LO and NLO kernels

$C(q_\perp)$ are proportional to the (quadratic) Casimir of the gauge group representation of the jet. The “leading order curves” in the plots are based on the full (unscreened) Eq. (21) at hard momenta, multiplied by $q_\perp^2/(q_\perp^2 + m_D^2)$ to make them merge smoothly with the analytic result Eq. (10) at low momenta, following the prescription given in [26]. The “next-to-leading order” curves use the leading order curves plus $C(q_\perp)^{(\text{NLO})}$ given by Eq. (19).

The NLO correction is already quite large for $\alpha_s = 0.1$, giving nearly a factor of 2 around $q_\perp \approx T$. As discussed in the introduction, this is consistent with the behavior observed for $\mathcal{O}(g)$ plasma effects in other quantities. At $\alpha_s = 0.3$, a typical value used in comparisons with RHIC data (see, e.g., [27]), it is clear that the strength of the correction has grown out of control, meaning that (presently unknown) yet higher-order corrections are most certainly also important (though our results suggest that the value of α_s required to fit the data could be significantly smaller than the estimate of [27]).

An interesting by-product of the approach used in this paper is that it extends naturally to higher orders: it makes perfect sense to evaluate the gauge-invariant Wilson loop Eq. (9) nonperturbatively within the *Euclidean* three-dimensional EQCD theory, as done perturbatively to $\mathcal{O}(g)$ in this paper, for instance using the lattice. Although this would not include *all* $\mathcal{O}(g^2)$ corrections to $C(q_\perp)$ (contributions from the hard scale $2\pi T$ will be missed), by analogy with the works on the pressure mentioned in the introduction, these missing contributions can be expected to be numerically subdominant [28]. We leave this possibility to future work.

B. Application to jet evolution

The dominant energy loss mechanism of high-energy particles (at weak coupling) is bremsstrahlung (including quark-antiquark pair production), triggered by soft collisions against plasma constituents. The theoretical description of these processes, at the leading order in the coupling,

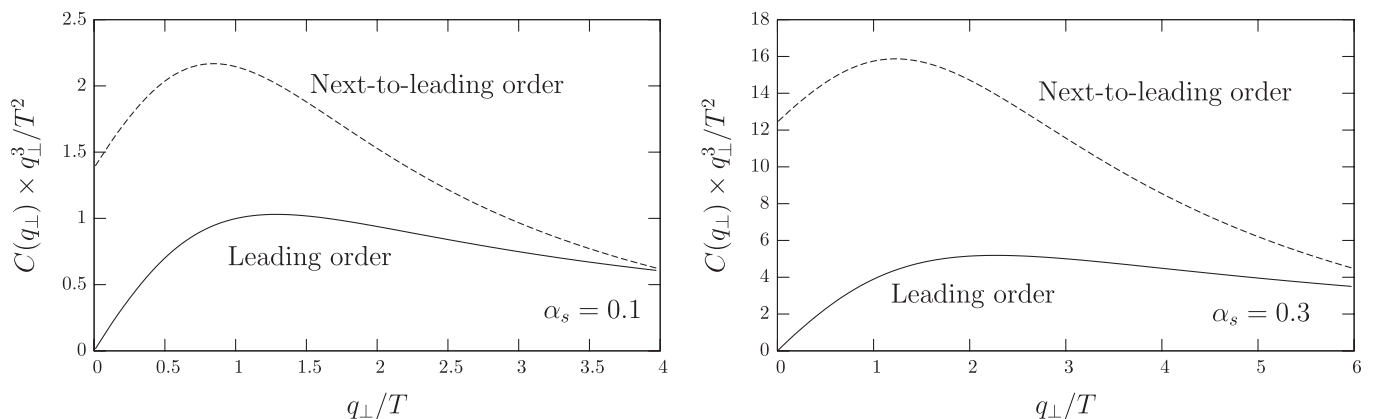


FIG. 1. LO and NLO collision kernels $C(q_\perp) \equiv (2\pi)^2 d\Gamma/d^2q_\perp$ for a fast quark in QCD (with $N_f = 3$ flavors), for $\alpha_s = 0.1$ and $\alpha_s = 0.3$. For gluons the curves are to be multiplied by a (Casimir) factor $9/4$.

is well established [29–31]. Their duration t_{form} depends on the energy of the participants, and interpolates between the Bethe-Heitler (single scattering) regime $t_{\text{form}} \sim E/q_{\perp}^2 \sim E/m_{\text{D}}^2$ at energies $E \lesssim T$, and the Landau-Pomeranchuk-Migdal (LPM) [32] (multiple-scattering) regime at high energies $E \gg T$ with $t_{\text{form}} \sim \sqrt{E/\hat{q}}$, in which destructive interference between different collisions plays a significant role.

In all of these regimes, however, the description factors into a “hard” collinear splitting vertex (Dokshitzer-Gribov-Lipatov-Altarelli-Parisi, DGLAP vertex [33]), times (the imaginary part of) a quantum mechanical amplitude (wave function in the transverse plane) which describes the in-medium evolution of the vertex. The latter accounts for the collisions which trigger, and occur during, the splitting process [29–31]. The DGLAP vertices themselves only involve hard scale physics (in essence, they are Clebsch-Gordon coefficients between different helicity states) and thus cannot receive $\mathcal{O}(g)$ corrections; the NLO effects, associated with soft classical fields having $p \sim gT$, are contained in the dressing amplitude.

In Sec. VI, we discuss these amplitudes at NLO and show that the relevant (three-body) collision kernel factors as a sum of the kernels $C(q_{\perp})$, exactly like it does at LO [29–31,34]. As a consequence, our results for $C(q_{\perp})$ can be used to give a full NLO treatment of radiative jet energy loss: one must simply include the NLO shift Eq. (19) to the two-body kernel $C(q_{\perp})$ which enters as an input to these calculations [35].

C. Momentum broadening coefficient (\hat{q})

When the effects of a large number of small collisions are added together, it is natural to replace them by an effective diffusive process. The diffusion coefficient relevant for transverse momentum broadening, \hat{q} , is the second moment of the collision kernel Eq. (1):

$$\hat{q} \equiv \int_0^{q_{\text{max}}} \frac{d^2 q_{\perp}}{(2\pi)^2} q_{\perp}^2 C(q_{\perp}). \quad (2)$$

The ultraviolet cutoff $|q_{\perp}| < q_{\text{max}}$ is needed to deal with the strong power-law tail $C(q_{\perp}) \sim g^4 T^3 / q_{\perp}^4$ at large q_{\perp} , which leads to a logarithmic dependence of \hat{q} on q_{max} . We emphasize that this is a *leading order* logarithm; below we shall comment on the value of the cutoff q_{max} . Using our NLO kernel Eq. (19), we have calculated the expansion of \hat{q} up to terms of order g^2 :

$$\begin{aligned} \frac{\hat{q}}{g^4 C_s T^3} &= \frac{C_A}{6\pi} \left[\log\left(\frac{T}{q^*}\right) + \frac{\zeta(3)}{\zeta(2)} \log\left(\frac{q_{\text{max}}}{T}\right) + C_b \right] \\ &+ \frac{N_f T_f}{6\pi} \left[\log\left(\frac{T}{q^*}\right) + \frac{3}{2} \frac{\zeta(3)}{\zeta(2)} \log\left(\frac{q_{\text{max}}}{T}\right) + C_f \right] \\ &+ \frac{C_A}{6\pi} \frac{m_{\text{D}}}{T} \xi^{(\text{NLO})} + \mathcal{O}(g^2), \end{aligned} \quad (3)$$

with $\xi^{(\text{NLO})} = \frac{3}{16\pi} (3\pi^2 + 10 - 4 \log 2) \simeq 2.1985$ a con-

stant calculated in Sec. V, characterizing the strength of the NLO correction. Here $m_{\text{D}}^2 = g^2 T^2 (C_A + N_f T_f) / 3$ is the leading order Debye mass, with $C_A = 3$ and $N_f T_f = 1.5$ in QCD with three flavors of quarks. The constants $C_b \simeq -0.068854926766592$ and $C_f \simeq -0.072856349715786$ are given in [26], to which we refer the reader for further discussion of the leading order result.

The series Eq. (3) represents the g expansion of $[1/(2\pi)$ times] the area under the curve in plots such as Fig. 1. For $\alpha_s = 0.1$ the area under the leading order curve in the figure (up to $q_{\text{max}} = 4T$) yields $\hat{q}^{\text{LO}} \simeq 2.60 \text{ GeV}^2/\text{fm}$ whereas the truncated expansion Eq. (3) gives $\hat{q}^{\text{LO,truncated}} \simeq 2.08 \text{ GeV}^2/\text{fm}$. The NLO shift is $\Delta\hat{q} \simeq 2.22 \text{ GeV}^2/\text{fm}$ from the figure, about a factor of 2 effect, and $\Delta\hat{q}^{\text{truncated}} \simeq 5.26 \text{ GeV}^2/\text{fm}$ according to Eq. (3). Thus Eq. (3) suffers from sizeable truncation errors. We would like to stress, however, that the NLO correction Eq. (19) itself, and Fig. 1, are not merely truncation errors from the lower-order contribution, but represent genuine NLO effects.

As discussed in the preceding subsection, it would be premature to attempt comparison of our \hat{q} results with experimental data, since it is clear that (yet unknown) higher-order corrections should also be important at physically relevant couplings. We also note that different approximation schemes taking \hat{q} as input [this excludes the AMY scheme [31,34], which uses the full $C(q_{\perp})$], when fitted to RHIC data, tend to disagree rather significantly on its preferred value [3]; since a critical analysis of these approximations lies beyond our scope, we simply conclude that it is not completely clear at present which experimentally extracted value of \hat{q} we should compare with.

It seems appropriate here to recall some subtleties associated with the phenomenological parameter \hat{q} , which do not arise if one instead works with the full collision kernel $C(q_{\perp})$. First, the value of the cutoff q_{max} to be used in Eq. (3) is process dependent: since the $q_{\perp} > q_{\text{max}}$ tail of $C(q_{\perp})$ describes collisions occurring on a finite rate [36] $\Gamma_{(q_{\perp} > q_{\text{max}})} \sim g^4 T^3 / q_{\text{max}}^2$, weighting them with q_{\perp}^2 in Eq. (22) ceases to make sense for $\Gamma_{(q_{\perp} > q_{\text{max}})}^{-1} \gtrsim t_{\text{jet}}$, with t_{jet} the jet’s lifetime, to be replaced with a formation time t_{form} for bremsstrahlung pairs in the context of energy loss calculations. Therefore, parametrically, one should set $q_{\text{max}} \sim \sqrt{g^4 T^3 t_{\text{jet}}}$. For bremsstrahlung in the deep LPM regime, $t_{\text{jet}} \rightarrow t_{\text{form}} \sim \sqrt{E/\hat{q}}$ so $q_{\text{max}} \sim g(ET^3)^{1/4}$ [37], which is parametrically much lower than the often-used kinematic cutoff $q_{\text{max}} \simeq (ET)^{1/2}$.

Second, the presence of the ultraviolet tail implies that collisions having $q_{\perp} \sim q_{\text{max}}$ (with q_{max} the physical cutoff as determined above), which are intrinsically nondiffusive, already contribute at the next-to-leading logarithm order to bremsstrahlung rates. That is, they contribute at $\mathcal{O}(1)$ compared to the log-enhanced diffusive contribution

$\sim \log q_{\max}/m_D$ due to $m_D \ll q_{\perp} \ll q_{\max}$. Therefore, approximations based on diffusive physics are, at best, expansions in inverse logarithms of the energy. The quality of such expansions has been studied in [37], with the conclusion that formulas to *next-to-leading* logarithm can be trusted at least when $E_{\text{jet}} \gtrsim 10T$ (E being the *smallest* energy of the participants), however their studies included the subleading term (e.g., the constant under the logarithm), which is not included in typical jet quenching calculations employing \hat{q} as an input parameter (see [3,38] and references therein for an overview of these approaches).

III. STRATEGY: SPACELIKE CORRELATORS AND EQCD

In this section, we relate certain correlators at space-time separation (more precisely, correlators supported on spacelike, and lightlike, hyperplanes of the type $x^0 = \tilde{v}x^3$, $\tilde{v} \leq 1$), to Euclidean-signature correlators. We will then apply to them the formalism of dimensional reduction.

A. Spacelike correlators

Field operators at spacelike separated points (anti)commute with each other and their correlator does not depend on the operator ordering. For two-point functions at vanishing time separation, a well-known Euclidean representation holds [39]

$$\begin{aligned} G_{ij}^{\tilde{v}}(t=0, \mathbf{x}) &\equiv \frac{1}{\text{Tr}e^{-\beta H}} \text{Tr}[e^{-\beta H} \mathcal{O}_i(\mathbf{x}) \mathcal{O}_j(0)] \\ &= T \sum_n \int \frac{d^3 \mathbf{p}}{(2\pi)^3} e^{i\mathbf{p} \cdot \mathbf{x}} G_E(\omega_n, \mathbf{p}), \end{aligned} \quad (4)$$

the sum running over the Matsubara frequencies $\omega_n = 2\pi i n T$, $\beta = 1/T$. G_{ij}^E is the Euclidean correlator of the operators $\mathcal{O}_{i,j}$, taken here to be bosonic.

In Lorentz-covariant theories, Eq. (4) can be extended immediately to any correlator which is equal time in a suitable boosted frame. Specifically, under a z -axis boost with velocity \tilde{v} , the thermal density matrix transforms to

$$e^{-\beta H} \rightarrow e^{-\tilde{\gamma} \beta (H' + \tilde{v} P^3)}, \quad (5)$$

the primed quantities referring to quantities in the boosted frame; $\tilde{\gamma} = \frac{1}{\sqrt{1-\tilde{v}^2}}$. The identification of H' and P^3 as the generators of time and space translation shows periodic identification $x'^{\mu} = x^{\mu} + i\tilde{\gamma}(\beta, -\tilde{v}\beta, 0_{\perp})$ for the geometry associated to Eq. (5), with associated quantization condition on the ‘‘Matsubara frequencies’’ $p'^0 + \tilde{v}p'^3 = 2\pi i n T / \tilde{\gamma}$. The spatial momentum p'^3 must be kept real: it serves as a label for the physical states living on the $x'^0 = 0$ hyperplane. Thus only the frequency p'^0 is complex. This determines the extension of Eq. (4) to equal-time, two-point functions in the boosted frame:

$$G_{ij}^{\tilde{v}}(x^0=0, \mathbf{x}') = \frac{T}{\tilde{\gamma}} \sum_n \int \frac{d^3 \mathbf{p}'}{(2\pi)^3} e^{i\mathbf{p}' \cdot \mathbf{x}'} G_E(p_n'^0, \mathbf{p}'), \quad (6)$$

with $p_n'^0 = -\tilde{v}p'^3 + 2\pi i n \frac{T}{\tilde{\gamma}}$.

It will be convenient to boost this formula back to the plasma rest frame and to write it for general space-time arguments, setting $\tilde{v} = \frac{x^0}{x^3}$:

$$G_{ij}^{\tilde{v}}(x^0, \mathbf{x}') = T \sum_n \int \frac{d^3 \mathbf{p}}{(2\pi)^3} e^{i p_n^0 x^0 - i \mathbf{p} \cdot \mathbf{x}'} G_E^E(p_n), \quad (7)$$

with $p_n^0 = 2\pi i n T$ and $p_n^3 = p^3 + 2\pi i n T \frac{x^0}{x^3}$.

Equation (7) is the main result of this section. It differs from Eq. (4) only due to the imaginary part of p_n^3 , which precisely guarantees that the Fourier exponential is a pure phase and that the sum over n makes sense. Equation (7) extends in a straightforward way to any higher-point correlator supported on $(\frac{x^0}{x^3} = \tilde{v})$ -type hyperplanes: one gets a summation integration $\sum_n \int_p$, with the p_n as in Eq. (7), for all external legs, subject to the usual restriction of momentum conservation (and of ‘‘ n conservation’’), like for equal-time, higher-point correlators [39]. The momenta running in loops must also be ‘‘twisted’’ like those in Eq. (7), e.g., $\text{Im} p^3 = \tilde{v} \text{Im} p^0$, to reflect the boosted-frame origin of the formula. This ensures that the imaginary part of every momentum is timelike, which is the natural domain for Euclidean physics.

We will be interested in the amplitudes of ultrarelativistic dipoles moving with velocity $v = 1$, e.g., $x^3 = x^0$ (note $\tilde{v} = 1/v$ in general). Our derivation of Eq. (7) might seem compromised, since an ‘‘infinite’’ boost with velocity $\tilde{v} = 1$ does not exist. However, a more careful look at the argument reveals that the boost plays no important role: after all we undid it in the end. All that is really important, is that we can imagine quantizing the system along hyperplanes parallel to \tilde{v} , and express the thermal density matrix within these hyperplanes. Since it is certainly possible to quantize a system along light fronts, the result Eq. (7) must hold for $x^3 = x^0$. An alternative derivation of this, based on sum rules, is sketched in the appendix.

The attentive reader might complain that setting $x^3 = x^0$ in Eq. (7) corresponds to taking a $v \searrow 1$ limit, whereas the physically relevant regime $v \nearrow 1$ lies beyond the reach of Eq. (7). Are we claiming that these limits are equivalent in general? No [40]. Our claim, explained in the introduction, is merely that they are equivalent for *classical* plasma physics effects. This is robust to the extent that only a phase-space suppressed fraction of the classical background fields propagate collinearly with the jet. This is true for the Coulomb field of the plasma particles, which track the particles but not the jet, but also for the plasma gluons, whose contribution to $C(q_{\perp})$ from the (unphysical) Čerenkov processes is readily checked to be proportional to $(v^2 - 1)$ and to smoothly vanish as $v \searrow 1$. It is unclear, however, whether this will remain true when quantum

effects are included (which will enter at order g^2), because of collinear components present in the jet's own wave function.

B. Dimensional reduction

Naturally, the contribution from soft physics (momenta $\sim gT$) to sums like Eq. (7) is expected to be dominated by the $n = 0$ mode. We thus begin by “integrating out” the modes with $n \neq 0$.

First we claim that loop diagrams for which all external momenta have $n = 0$ are equal to the standard ones. These two sets of diagrams have $p^0 = 0$ and p_z real, and could only differ due to the twisted Matsubara momenta Eq. (7) which circulate in the former; our claim is that this does not affect their value. The reason is that the imaginary part of every momentum P in such loops is timelike with a real part obeying $\text{Re}p^0 = 0$, ensuring that $\text{Re}P^2$ is positive definite (spacelike). The imaginary part of the p^3 integration contours can thus be deformed from $\text{Im}p^3 = \tilde{v} \text{Im}p^0$ to $\text{Im}p^3 = 0$ without crossing any pole.

In particular, the modes having $n = 0$ are described by precisely the standard EQCD three-dimensional effective theory [41,42]. EQCD is pure three-dimensional Yang-Mills with coupling constant $g_{3D}^2 = g^2 T$ coupled to a massive adjoint scalar A_0 of mass m_D . It is an effective theory for the gT scale (the Euclidean version of the hard thermal loop theory [14]), in which the loop expansion proceeds in powers of $g^2 T/m_D \sim g$. Its parameters do not receive $\mathcal{O}(g)$ corrections.

The propagators of EQCD are

$$\tilde{G}^{00}(q) = \frac{-1}{q^2 + m_D^2}, \quad \tilde{G}^{ij}(q) = \frac{\delta^{ij}}{q^2} - \frac{\xi q^i q^j}{q^4}. \quad (8)$$

(We use the tilde to denote that these are three-dimensional propagators.) The minus sign in front of the A_0 propagator reflects the fact that we will couple it to Minkowski-space Wilson lines: we have *not* performed a Wick rotation.

In addition to its interaction with the $n = 0$ modes, we must also include the direct coupling of the operator of interest to the $n \neq 0$ modes. Physically, and as shown in the appendix, a contribution from these modes would correspond, in the real-time formalism, to a failure of the soft approximation $n_B(p^0) \approx T/p^0$. Such a failure would signal a contribution from the $p^0 \sim T$ region in Minkowski space, which would necessary be signaled by ultraviolet divergences in the soft approximation, since this approximation correctly describes the intermediate region $gT \ll p^0 \ll T$ and any contribution from the scale T should leave an imprint on this region. Thus, provided we do not find ultraviolet divergences from the $n = 0$ contribution alone (which computes exactly the soft approximation, see the appendix), we conclude that we can safely ignore the direct coupling to the $n \neq 0$ modes. This will turn out to be our case.

IV. THE CALCULATION

In this section, we express the collision kernel $C(q_\perp)$ as a correlator supported on $x^3 = x^0$ trajectories and evaluate it using EQCD. We only give details in the Feynman gauge $\xi = 0$; as a check on the calculation, however, we explicitly checked the ξ independence of $C(q_\perp)$.

A. Operator definition of $C(q_\perp)$ and leading order result

The evolution of the transverse momentum of a high-energy particle can be described by looking at its density matrix. For classical effects, however (and even more so because we are taking the velocity to be $v = 1 + \epsilon$), we can neglect operator ordering issues and replace the evolution of a density matrix by that of a dipole. We will come back to operator ordering issues in Sec. VI B.

A high-energy dipole ($E \gg m_D$) propagates eikonally in the soft classical background. The collision kernel describing the evolution of its transverse momentum can thus be recovered from the Fourier transform of the (long-time limit of the) dipole propagation amplitude W [29,30,43]:

$$W(t, x_\perp) \sim e^{iC(x_\perp) + \mathcal{O}(1)}, \quad t \rightarrow \infty, \quad (9)$$

$$C(q_\perp) \equiv \int d^2 x_\perp e^{ip_\perp \cdot x_\perp} C(x_\perp).$$

$C(q_\perp)$ is short for $(2\pi)^2 d\Gamma/d^2 q_\perp$, as in Eq. (1). The dipole amplitude $W(t, x_\perp)$ is given by the trace of a long, thin rectangular Wilson loop stretching along the light-cone coordinate x^+ , with a small transverse extension x_\perp (see Fig. 2).

The naive dimensional reduction of the Wilson loop Eq. (9) yields a Wilson loop stretching along the z axis of the three-dimensional EQCD theory. It couples to the linear combination $A_+ = (A_z + A_0)$ of the EQCD fields, reflecting its ultrarelativistic origin. This “naive” dimensional reduction corresponds to keeping only the direct coupling to the $n = 0$ modes. As explained in Sec. III B, this will be justified provided we do not find ultraviolet divergences.

At the lowest order in perturbation theory, only the single-gluon exchange diagram (Fig. 3(a)) contributes,

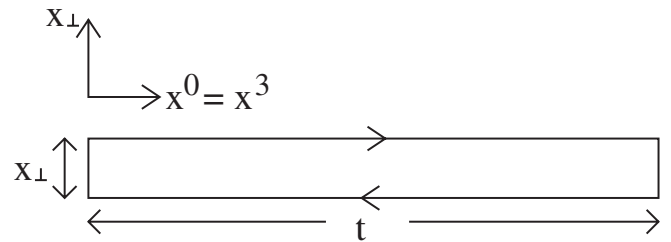
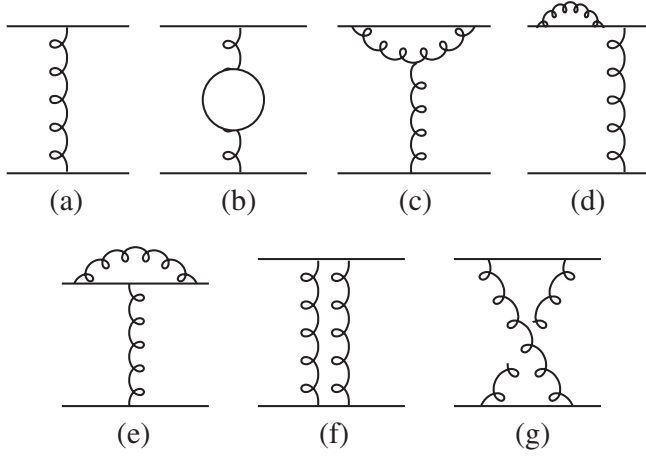


FIG. 2. Wilson loop representation of the dipole amplitude.

FIG. 3. Tree and one-loop diagrams contributing to $C(q_\perp)$.

$$C(q_\perp) = g^2 T C_s \int_{-\infty}^{\infty} dz \int d^2 x_\perp e^{i p_\perp \cdot x_\perp} \tilde{G}_{++}(z, x_\perp) \\ = g^2 T C_s \left(\frac{1}{q_\perp^2} - \frac{1}{q_\perp^2 + m_D^2} \right), \quad (10)$$

where we have used Eq. (8), with $q_z = 0$ as a result of the z integration. The compact form Eq. (10) was first obtained by means of sum rules by Aurenche, Gelis and Zaraket [18], which is shown in the appendix to be equivalent to the present approach.

B. Figure 3(b)

At the next-to-leading order (one-loop), self-energy insertions to single-gluon exchange, Fig. 3(b), contribute [we will often write q_\perp for a three-vector with $q_z = 0$, which should cause no confusion; \int_p is short for $\int \frac{d^3 p}{(2\pi)^3}$]:

$$\frac{C(q_\perp)_{(b)}}{g^2 T C_s} = \frac{\delta \Pi^{00}(q_\perp)}{(q_\perp^2 + m_D^2)^2} - \frac{\delta \Pi^{zz}(q_\perp)}{q_\perp^4}, \\ \frac{\delta \Pi^{00}(q)}{g^2 T C_A} = \int_p \left[\frac{-(2q_\perp - p)^2}{p^2((q_\perp - p)^2 + m_D^2)} + \frac{3}{p^2} \right], \\ \frac{\delta \Pi^{zz}(q)}{g^2 T C_A} = \int_p \left[\frac{-2p_z^2}{(p^2 + m_D^2)((q_\perp - p)^2 + m_D^2)} + \frac{1}{p^2 + m_D^2} \right] \\ + \int_p \left[\frac{-3p_z^2 - 2q_\perp^2 - p^2}{p^2(q_\perp - p)^2} + \frac{2}{p^2} + \frac{p_z^2}{p^2(q_\perp - p)^2} \right]. \quad (11)$$

Each bracket includes the contributions of one fish and one tadpole diagram, while the last one also includes the ghost loop.

The (linear) ultraviolet divergences in Eq. (11) are to be canceled by matching counterterms that can be unambiguously calculated within the framework of dimensional reduction [41,42]. They merely represent the (hard thermal loop) coupling of the $n \neq 0$ gluons to the soft $n = 0$ ones,

e.g., the gluon contribution to the A^0 mass squared m_D^2 . The fact that the direct coupling to exchange gluons with $q^0 = q^3 \neq 0$ does not contribute to the divergences can also be checked explicitly, from the convergence, with respect to q^3 , of the real-time integral Eq. (21) (this justifies making the soft approximation on q^0). Thus the divergences in Eq. (11) do not signal the presence of “new contributions” beyond the EQCD effective theory, as discussed in Sec. III B.

Employing dimensional regularization, the divergences simply go away [44] and the counterterms are zero to $\mathcal{O}(g)$ [42]. This way we obtain (all our arctangents run from 0 to $\pi/2$)

$$\frac{C(q_\perp)_{(b)}}{g^4 T^2 C_s C_A} = \frac{-m_D - 2 \frac{q_\perp^2 - m_D^2}{q_\perp} \tan^{-1}(\frac{q_\perp}{m_D})}{4\pi(q_\perp^2 + m_D^2)^2} + \frac{7}{32q_\perp^3} \\ + \frac{m_D - \frac{q_\perp^2 + 4m_D^2}{2q_\perp} \tan^{-1}(\frac{q_\perp}{2m_D})}{8\pi q_\perp^4}. \quad (12)$$

C. Figure 3(c)

Figure 3(c) plus its permutation contribute

$$\frac{C(q_\perp)_{(c)}}{g^4 T^2 C_s C_A} = \int_p \left[\frac{2}{q_\perp^2(p^2 + m_D^2)((q_\perp - p)^2 + m_D^2)} \right. \\ \left. - \frac{2}{(q_\perp^2 + m_D^2)(p^2 + m_D^2)(q_\perp - p)^2} \right] \quad (13) \\ = \frac{-\tan^{-1}(\frac{q_\perp}{m_D})}{2\pi q_\perp(q_\perp^2 + m_D^2)} + \frac{\tan^{-1}(\frac{q_\perp}{2m_D})}{2\pi q_\perp^3}. \quad (14)$$

In the Feynman gauge there is no contribution involving only transverse gauge fields because such a contribution would involve the (trivial) zzz vertex. Equation (13) is manifestly convergent.

D. Figures 3(d)–3(g)

Our calculation is based on a quasiparticle expansion, e.g., we simply set on shell the external legs of scattering diagrams. The relevant expansion parameter is g , e.g., the ratio of the scattering width $\sim g^2 T$ to the scattering’s natural frequency scale m_D . Thus in evaluating the external state corrections Fig. 3(d) we need only keep those effects which are not suppressed by the smallness of the width. A narrow resonance being described by just its position and the total area under it, this means that Fig. 3(d), at $\mathcal{O}(g)$, produces only mass-shell corrections and wave function renormalization factors. The (here imaginary) “mass-shell” corrections have no effects: they are identical for the initial and final states, so the “energy” (z momentum) transfer is zero in any case. The wave function renormalization contribution is given by an energy derivative of the

eikonal self-energy, and Fig. 3(e) is unambiguous, yielding, respectively, (including all figures of similar topology):

$$\begin{aligned} \frac{C(q_\perp)_{(d)}}{g^4 T^2 C_s} &= 2C_s \tilde{G}_{++}(q_\perp) \int_p \tilde{G}_{++}(p) \frac{d}{dp_z} \frac{1}{p_z - i\epsilon}, \\ \frac{C(q_\perp)_{(e)}}{g^4 T^2 C_s} &= 2\left(C_s - \frac{1}{2}C_A\right) \tilde{G}_{++}(q_\perp) \int_p \frac{\tilde{G}_{++}(p)}{(p_z - i\epsilon)^2}. \end{aligned} \quad (15)$$

The sum of Figs. 3(d) and 3(e) is proportional to C_A and identically vanishes in the Abelian theory ($C_A = 0$), as required by Abelian exponentiation [45].

Part of Fig. 3(f) is already included by the exponentiation of Eq. (10) (Fig. 3(a)): this generates the approximation to Fig. 3(f) in which the intermediate eikonal propagators are put on shell. To avoid double counting, this must be subtracted. We must first regulate the associated ‘‘pinching’’ ($q_z \rightarrow 0$) singularity, which we do by flowing a small external z momentum ω into the Wilson loop. We then take the limit $\omega \rightarrow 0$ after the subtraction. Figure 3(g) poses no difficulty.

$$\begin{aligned} \frac{C(q_\perp)_{(f)}}{g^4 T^2 C_s} &= C_s \int_p \tilde{G}_{++}(p) \tilde{G}_{++}(q-p) \\ &\times \lim_{\omega \rightarrow 0} \left[\frac{1}{(p_z + i\epsilon)(p_z + \omega - i\epsilon)} \right. \\ &\left. + \frac{2\pi i \delta(p_z)}{\omega - i\epsilon} \right], \end{aligned} \quad (16)$$

$$\frac{C(q_\perp)_{(g)}}{g^4 T^2 C_s} = -\left(C_s - \frac{1}{2}C_A\right) \int_q \frac{\tilde{G}_{++}(p) \tilde{G}_{++}(q_\perp - p)}{(p_z - i\epsilon)^2}. \quad (17)$$

Equation (16) has a well-defined $\omega \rightarrow 0$ limit, as follows from the identity $1/(p_z + i\epsilon) - 1/(p_z - i\epsilon) = -2\pi i \delta(p_z)$. This limit takes a form identical to Eq. (17) and the sum is proportional to C_A , again as required by Abelian exponentiation. This confirms that our evaluation of Fig. 3(f) is indeed correct.

In summary, Figs. 3(d)–3(g) produce

$$\frac{C(q_\perp)_{(d)-(g)}}{g^4 T^2 C_s C_A} = \int_p \frac{\tilde{G}_{++}(p) \tilde{G}_{++}(q_\perp - p) - 2\tilde{G}_{++}(p) \tilde{G}_{++}(q_\perp)}{2(p_z - i\epsilon)^2} = \frac{m_D}{4\pi(q_\perp^2 + m_D^2)} \left[\frac{3}{q_\perp^2 + 4m_D^2} - \frac{2}{(q_\perp^2 + m_D^2)} - \frac{1}{q_\perp^2} \right]. \quad (18)$$

The function \tilde{G}_{++} is $\tilde{G}_{00} + \tilde{G}_{zz}$ as given in Eq. (8). To evaluate the integral we found it convenient to first apply integration by parts to the $1/(p_z - i\epsilon)^2$ denominator, which removes the explicit p_z dependence and reduces the integral to a set of standard isotropic Feynman integrals. This contribution is manifestly infrared- (and ultraviolet-) safe, upon enforcing $p \leftrightarrow (q_\perp - p)$ symmetry.

E. Final formulas

In summary, we have obtained all $\mathcal{O}(g)$ contributions to the collision kernel $C(q_\perp)$:

$$\begin{aligned} C(q_\perp)^{(\text{LO})} &= \frac{g^2 T C_s m_D^2}{q_\perp^2 (q_\perp^2 + m_D^2)}, \\ \frac{C(q_\perp)^{(\text{NLO})}}{g^4 T^2 C_s C_A} &= \frac{7}{32q_\perp^3} + \frac{-3m_D - 2\frac{q_\perp^2 - m_D^2}{q_\perp} \tan^{-1}\left(\frac{q_\perp}{m_D}\right)}{4\pi(q_\perp^2 + m_D^2)^2} + \frac{m_D - \frac{q_\perp^2 + 4m_D^2}{2q_\perp} \tan^{-1}\left(\frac{q_\perp}{2m_D}\right)}{8\pi q_\perp^4} \\ &\quad - \frac{\tan^{-1}\left(\frac{q_\perp}{m_D}\right)}{2\pi q_\perp (q_\perp^2 + m_D^2)} + \frac{\tan^{-1}\left(\frac{q_\perp}{2m_D}\right)}{2\pi q_\perp^3} \\ &\quad + \frac{m_D}{4\pi(q_\perp^2 + m_D^2)} \left[\frac{3}{q_\perp^2 + 4m_D^2} - \frac{1}{q_\perp^2} \right]. \end{aligned} \quad (19)$$

These expressions are valid for $q_\perp \ll T$. The leading order kernel for $q_\perp \gtrsim T$ gets slightly modified; see Eq. (21) below.

The appearance of arctangents with two distinct arguments in Eq. (19) can be understood by looking in the complex q_\perp^2 plane: $\tan^{-1}(q_\perp/2m_D)$ has a branch cut starting at $q_\perp^2 = -4m_D^2$ and represents the exchange of a pair of two quanta of mass m_D (longitudinal gluons), while the branch cut of $\tan^{-1}(q_\perp/m_D)$ starts at $q_\perp^2 = -m_D^2$ and represents the exchange of one longitudinal and one transverse gluon. Both arctangents occur since both of these

pairs of states can be exchanged. Exchange of two massless quanta also occurs, and generates $1/\sqrt{q_\perp^2}$ -type of discontinuities instead of arctangents.

V. EVALUATION OF $\hat{q}^{(\text{NLO})}$

The effective theory approach we have used so far is valid for $q_\perp \ll T$. As mentioned in Sec. II C, however, the momentum broadening coefficient \hat{q} [second moment of $C(q_\perp)$] receives contributions from all scales up to a

process-dependent cutoff q_{\max} . In this section, we will assume $q_{\max} \gg T$.

To separate the soft and hard contributions to \hat{q} , we find it convenient to introduce an auxiliary scale q^* obeying $m_D \ll q^* \ll T$:

$$\hat{q} = \int_0^{q^*} \frac{d^2 q_{\perp}}{(2\pi)^2} q_{\perp}^2 C(q_{\perp})^{\text{soft}} + \int_{q^*}^{q_{\max}} \frac{d^2 q_{\perp}}{(2\pi)^2} q_{\perp}^2 C(q_{\perp})^{\text{hard}}. \quad (20)$$

The soft kernel $C(q_{\perp})^{\text{soft}}$ is given by Eq. (19). The hard kernel $C(q_{\perp})^{\text{hard}}$ describes tree-level $2 \rightarrow 2$ scattering processes against plasma constituents, with self-energy corrections omitted on the exchange gluon (since they represent only $\sim g^2$ corrections for $q_{\perp} \sim T$). The large particle energy $E \gg T$ guarantees that the Mandelstam invariants $s \sim ET$ and $-t = q_{\perp}^2$ obey $|t| \ll s$, so that the relevant scattering matrix elements assume the universal (eikonal) form $\propto s^2/t^2$. The kinematics force $q^0 = q_z$ for the momentum transfer q . In fact, these processes are precisely described by the central cut of (a four-dimensional version of) Fig. 3(b). Performing the q_z integration in the expression for the collision rate (as done in [17]; more details can be found in [26]), one obtains

$$C(q_{\perp})^{\text{hard}} = \frac{g^4 C_s}{q_{\perp}^4} \int \frac{d^3 p}{(2\pi)^3} \frac{p - p_z}{p} [2C_A n_B(p)(1 + n_B(p')) + 4N_f T_f n_F(p)(1 - n_F(p'))], \quad (21)$$

with p, p' the initial and final momentum of the target particle; $p' = p + q_z$, $q_z = q^0 = \frac{q_{\perp}^2 + 2q_{\perp} \cdot p}{2(p - p_z)}$. In the regime $q_{\perp} \ll T$, $p' \approx p$ and Eq. (21) reduces (as it must) to the large q_{\perp} limit of Eq. (10), $C(q_{\perp}) \approx g^2 m_D^2 C_s T / q_{\perp}^4$.

Integrating Eq. (21) over q to obtain the hard contribution to Eq. (20), and expanding it in powers of q^*/T , yields

$$\begin{aligned} \frac{\hat{q}^{\text{hard}}}{g^4 C_s T^3} &= \frac{C_A}{6\pi} \left[\log\left(\frac{T}{q^*}\right) + \frac{\zeta(3)}{\zeta(2)} \log\left(\frac{q_{\max}}{T}\right) + C_b \right] \\ &+ \frac{N_f T_f}{6\pi} \left[\log\left(\frac{T}{q^*}\right) + \frac{3}{2} \frac{\zeta(3)}{\zeta(2)} \log\left(\frac{q_{\max}}{T}\right) + C_f \right] \\ &+ \frac{C_A}{6\pi} \frac{3}{16} \frac{q^*}{T} + \dots \end{aligned} \quad (22)$$

with the omitted terms suppressed by $(q^*/T)^2$ or more. We have verified by numerical integration the first five significant digits of the numerical constants C_g, C_f , as quoted below Eq. (3) from the results of [26,46]. The $\sim q^*/T$ term arises from soft bosons with $p, p' \ll T$ and can be obtained in the soft approximation $n_B(p), n_B(p') \rightarrow T/p, T/p'$; it is also given in [26].

The soft contribution to Eq. (20), e.g., the second moment of Eq. (19), admits the expansion

$$\begin{aligned} \frac{\hat{q}^{\text{soft}}}{C_s} &= \frac{g^4 T^2 C_A m_D}{2\pi} \left[-\frac{q^*}{16m_D} + \frac{3\pi^2 + 10 - 4\log 2}{16\pi} \right] \\ &+ \frac{m_D^2 g^2 T}{2\pi} \log\left(\frac{q^*}{m_D}\right) + \dots \end{aligned} \quad (23)$$

with the omitted terms being suppressed by powers of m_D/q^* . The q^* dependence of Eq. (22) and (23) cancels out in their sum, as it must do, producing the claimed formula Eq. (3). This cancellation is a nontrivial check on the calculation.

The reader might inquire as to whether we have consistently included all $\mathcal{O}(g)$ contributions to \hat{q} . Taking $q^* \sim g^{1/2}T$, for instance, the omitted terms $\sim (q^*/T)^2$ in Eq. (22) might naively appear to be $\mathcal{O}(g)$, suggesting contributions from other, omitted terms. Estimates of this kind can be misleading, however, because q^* is not a physical scale in this problem. The matching region $m_D \ll q^* \ll T$ can be described equivalently using the low-energy description (EQCD) or the full theory, ensuring that q^* always disappears from final expressions. This is seen explicitly for the leading truncation errors $\sim q^*/T$ in Eqs. (22) and (23): instead of producing $\mathcal{O}(g^{1/2})$ corrections, as one would naively expect setting $q^* \sim g^{1/2}T$, they cancel against each other and the leading correction is $\mathcal{O}(g)$ not $\mathcal{O}(g^{1/2})$. Since similar cancellations are bound to occur at all orders, this simply means that the scale q^* should not enter power-counting estimates. Because higher loop diagrams are $\sim g^2$ when $q_{\perp} \sim T$ and because we have included all $\mathcal{O}(g)$ effects when $q_{\perp} \sim m_D$, we thus conclude that we have included all $\mathcal{O}(g)$ contributions.

Finally, we note that, in the spirit of [47], we could have used dimensional regularization to separate the q integration, instead of the sharp cutoff q^* . In this scheme, the hard q^*/T term in Eq. (22) disappears: there is no suitable dimensional parameter to replace q^* . The $\mathcal{O}(g)$ corrections then come solely from the (unambiguous) dimensionally regulated soft integral Eq. (19).

VI. JET EVOLUTION

We now extend the calculation, which so far had been concerned with momentum broadening, to obtain the collision kernel relevant for bremsstrahlung and pair production processes. The new complication is that, except for QED processes, the relevant object to evolve in the plasma is no longer a ‘‘dipole’’ but involves three charged states. For instance, to describe the gluon bremsstrahlung process $\psi \rightarrow g\psi$, one must evolve an operator which annihilates a quark and creates a quark-gluon pair (see [29–31], which, however, use somewhat different notations):

$$\mathcal{O}_{\psi \rightarrow \psi g} = |\psi, g\rangle\langle\psi|. \quad (24)$$

The three color charges in Eq. (24) are paired together to form a color-singlet state, as dictated by the (DGLAP) gluon emission vertex which generates this operator.

Only one transverse momentum suffices to describe the internal state of Eq. (24), as a consequence both of momentum conservation and of rotational symmetry: by suitably choosing the z axis it is always possible to “gauge” to zero one of the transverse momenta [see the discussion preceding Eq. (6.6) in [31,48]]. In the following, for concreteness, we shall gauge to zero the transverse momentum of particle 1 and q_\perp will refer to the transverse momentum of particle 2.

At the leading order, the relevant collision kernel is a sum over two-body contributions [29–31]:

$$\begin{aligned} \frac{d\Gamma_3(q_\perp)}{d^2q_\perp/(2\pi)^2} &= \frac{C_2 + C_3 - C_1}{2} \tilde{C}(q_\perp) \\ &+ \frac{C_1 + C_3 - C_2}{2} \tilde{C}\left(\frac{E_1}{E_2} q_\perp\right) \\ &+ \frac{C_1 + C_2 - C_3}{2} \tilde{C}\left(\frac{E_1}{E_3} q_\perp\right) \end{aligned} \quad (25)$$

with C_i and E_i , respectively, the Casimir and longitudinal momenta of the participating particles; $\tilde{C}(q_\perp) \equiv \frac{1}{C_s} C(q_\perp)$ denotes a single-particle collision kernel with its Casimir factor stripped off; we recall that the LO (and NLO) kernels respect Casimir scaling. In the special limit in which one of the E_i becomes much smaller than the other ones, the motion of this particle dominates and the kernel Eq. (25) reduces to the one for single-particle diffusion, $C(q_\perp)$, for $i = 2, 3$, and $C(\frac{E_1}{E_2} q_\perp)$ when $i = 1$.

As we presently show, it turns out that the formula Eq. (25) also holds at NLO, provided the NLO expression Eq. (19) for $C(q_\perp)$ is used in it.

A. “Three-pole” propagation at NLO

To keep the discussion simple we will assume that particle 3 is a gluon (or any color adjoint state), which is sufficient to cover all splitting processes in QCD (and $\mathcal{N} = 4$ super Yang-Mills). This ensures that particles 1 and 2 are antiparticles to each other. We denote by $|s\rangle$ the relevant singlet state in the tensor product of the three charges; explicitly, $|s\rangle$ is given by the representation matrices $(t_1)_ij^a$.

The already-treated “dipole” Figs. 3(a)–3(g) must now be summed over the three possible pairs of particles, and we must recompute their group theory factors. Figures 3(a) and 3(b) involve, in the case the interaction is between particles 1 and 2 [31],

$$\begin{aligned} -\langle s|t_1^a \otimes t_2^a|s\rangle &= \langle s|\frac{t_1^a t_1^a + t_2^a t_2^a - (t_1 + t_2)^a (t_1 + t_2)^a}{2}|s\rangle \\ &= \frac{C_1 + C_2 - C_3}{2}, \end{aligned} \quad (26)$$

which reproduces the structure Eq. (25), upon summing over pairs and using rotational invariance to gauge to zero

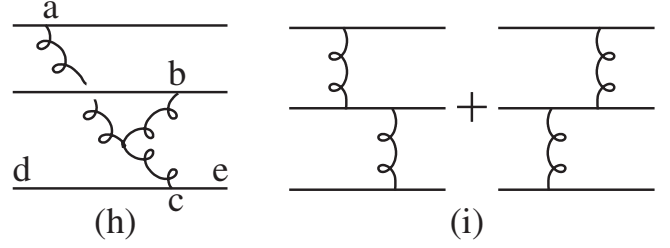


FIG. 4. Additional diagrams for the evolution of a triplet of charges.

particle 1’s \perp momentum. Figures 3(c)–3(g) fit the same structure, as follows from the fact that they organize themselves into commutators. For instance,

$$\begin{aligned} (c) &\propto i f^{abc} \langle s|t_1^a t_1^b \otimes t_2^c|s\rangle = -\frac{C_A}{2} \langle s|t_1^a \otimes t_2^a|s\rangle, \\ (f) + (g) &\propto \langle s|[t_1^a, t_1^b] \otimes \frac{[t_2^a, t_2^b]}{2}|s\rangle = -\frac{C_A}{2} \langle s|t_1^a \otimes t_2^a|s\rangle. \end{aligned} \quad (27)$$

Here we have used the identities $[t^a, t^b] = i f^{abc} t^c$ and $f^{abc} f^{abc'} = C_A \delta^{cc'}$.

There are also new diagrams (Fig. 4), which couple together the three particles nontrivially. In Fig. 4(h), the Yang-Mills 3-vertex generates a factor f^{abc} and the coupling to the gluon line is given by $(t_3)_{de}^c \propto f^{cde}$, whence

$$(h) = \langle s|t_1^a t_2^b t_3^c|s\rangle f^{abc} \propto \text{Tr}_1(t^a t^d t^b t^e) f^{abc} f^{dec} = 0, \quad (28)$$

with the trace taken in the representation of the particle 1. We could prove this identity by making extensive use of the antisymmetry of the f^{abc} . Figures 4(i) are similar to Fig. 3(g) treated in Sec. IV D, and the main point is that there is a sign between the two figures, due to the reversed middle propagator, thus yielding zero:

$$(i) \propto \langle s|t_1^a \otimes [t_2^a, t_2^b] \otimes t_3^b|s\rangle = 0. \quad (29)$$

Thus the new Figs. 4(h) and 4(i) vanish and the factorization formula Eq. (25) remains valid at NLO. We view this as somewhat surprising and believe it could be an artefact of the relatively low order in perturbation theory to which we are working.

B. Operator ordering

We now briefly discuss operator ordering issues, for the Wilson lines in Eq. (9) and their three-particle generalization Eq. (24). Although this is not directly relevant to the purely classical effects which are the main object of this paper, because nonperturbative definitions of \hat{q} have been used in the literature [19,21] we feel that a discussion of them can be of interest.

To help clarify the physical significance of these issues, let us first consider, in QED, the processes of photon

bremsstrahlung from a charge, and of pair production from a photon. These processes differ in that the former takes place within the electromagnetic field generated by the initial charge, but the latter takes place in an essentially undisturbed medium (the induced field being suppressed by the small size of the produced dipole). The collision kernels relevant to these two processes could thus be different, due to the different backgrounds, and should be defined differently. In the eikonal regime it is the role of the Wilson lines trailing behind the charges to account for these effects, which requires however that they be properly ordered.

The proper ordering can be readily described using the language of the Schwinger-Keldysh “doubled fields” [49], in which amplitudes and their complex conjugate are described by type-1 and type-2 fields, respectively. For photon bremsstrahlung, evolving the relevant $|\psi\gamma\rangle\langle\psi|$ matrix element clearly requires one type-1 ψ (and γ) and one type-2 $\bar{\psi}$ field, whereas for pair production, evolving $|\psi\bar{\psi}\rangle\langle\gamma|$ requires both charged fields to be type-1 (and γ to be type-2). In the latter case the Wilson lines nearly cancel against each other (for a small dipole), whereas in the former case they fail to cancel, due to operator ordering issues (they live on different branches of the Keldysh contour): instead they source an electromagnetic field. This reproduces the expected physics.

The story for QCD must be similar: for instance, evolving a $|\psi, g\rangle\langle\psi|$ operator, relevant for gluon bremsstrahlung, should require type-1 ψ and g fields, and a type-2 $\bar{\psi}$ field, with the obvious replacements to be made for other processes. Thus the strong coupling calculations of the momentum broadening coefficient in [21,22], strictly speaking, gives a \hat{q} applicable to *photon* bremsstrahlung, whereas the “jet quenching parameter” defined in [19], being defined from a spacelike limit of correlators, is by hypothesis independent of operator ordering.

It is not clear, at least to the author, the extent to which these effects can be numerically important. Obviously, at weak coupling, they are suppressed by a power of the coupling (the preceding subsection shows that the suppression is at least $\sim g^2$). Furthermore, in the $v \nearrow 1$ limit relevant to high-energy jets, an argument based on the shrinking down of the “causal diamond” enclosing any two points on the trajectory of the jet might suggest that these effects disappear—e.g., there is no time available for the induced field to influence the jet back; a rigorous analysis, in particular, of quantum effects, will not be attempted here.

ACKNOWLEDGMENTS

I am indebted to Guy D. Moore for useful discussions, and to P. Arnold and W. Xiao for sharing an early draft of their work [26]. This work was supported in part by the Natural Sciences and Engineering Research Council of Canada.

APPENDIX A: RELATION TO SUM RULES

In this appendix, we consider the problem of calculating, directly in four dimensions, the collision kernel Eq. (9):

$$C(q_\perp)/g^2 C_s = \int \frac{dq_z}{2\pi} G_{++}^>(q^0 = q_z, q_\perp) \quad (\text{A1})$$

with $q_\perp \ll T$, and G_{++} the full HTL-resummed propagator [14]. The strategy pursued in this work may be considered a next-to-leading order extension of the sum rule of Aurenche, Gelis and Zaraket (AGZ) [18], and here we aim to show the equivalence, at the leading order, of our formalisms.

1. Sum rules and causality

First, we relate the AGZ sum rules to Lorentz-covariant causality, which implies that retarded correlators $G^R(Q)$ are analytic functions of the four-momentum Q when a positive timelike or lightlike imaginary four-vector is added to it. This statement extends, in a Lorentz-covariant way, the familiar analyticity of G^R in the upper-half q^0 plane. Lightlike imaginary parts are also allowed because causality is preserved along light fronts (e.g., $G^R(x^+)$ vanishes for negative light-cone time x^+).

In the classical approximation $n_B(q^0) \approx T/q^0$, Eq. (A1) becomes

$$\begin{aligned} (\text{A1}) = T \int \frac{dq_z}{2\pi} \\ \times \frac{G_{++}^R(q^0 = q_z, q_\perp) - G_{++}^A(q^0 = q_z, q_\perp)}{q_z}. \end{aligned} \quad (\text{A2})$$

To evaluate this by contour integration we first displace the $q_z = 0$ pole slightly off axis, $1/q_z \rightarrow 1/(q_z - i\epsilon)$, which does not change the result since $(G^R - G^A)$ vanishes at $q_z = 0$. Next, we note, using the standard HTL expressions [14], that $G_{++}^{R,A}$ vanishes (like $1/q_z^2$) at large $|q_z|$, making it possible to close integration contours at infinity. Closing the contour for G^R (respectively, G^A) in the upper (respectively, lower) half-plane, one obtains a unique residue $iTG_{++}^R(q^0 = q_z = 0, q_\perp)$ from G^R and nothing from G^A , due to their aforementioned analyticity properties, thus reproducing Eq. (10):

$$\text{Eq. (A1)} = T \left(\frac{1}{q_\perp^2} - \frac{1}{q_\perp^2 + m_D^2} \right). \quad (\text{A3})$$

Additional poles at the Matsubara frequencies $q^0 = q_z = 2\pi inT$ would have appeared in this result, in agreement with the sum Eq. (7), had we kept the full Bose distribution function $n_B(q^0)$. In particular this shows that the classical approximation to distribution functions is equivalent to keeping only the $n = 0$ Matsubara frequency.

2. AGZ's sum rule

AGZ [18] study exactly the integral Eq. (A1), but parametrized using a different variable, $x = q^0/q$ (so that $q^0(x) = q_z(x) = |q_\perp| |x/\sqrt{1-x^2}$):

$$(A1) = |q_\perp| \int_{-1}^1 \frac{dx}{2\pi(1-x^2)^{3/2}} G_{++}^>(x, q_\perp). \quad (A4)$$

A key observation in [18] is that the HTL propagators, viewed as a function of x with q_\perp fixed and $q^0 = q_z$, are analytic in the whole complex x plane, apart from a branch cut at real $x \in [-1, 1]$. Using methods of complex analysis, they could then derive the result Eq. (A3).

To show that this analyticity property in x is equivalent to the analyticity in q^+ that we have just used (e.g., to causality), we rewrite the change of variable above Eq. (A4) as

$$q^0(x) = q_z(x) = i|q_\perp| \frac{x}{\sqrt{x^2-1}}, \quad (A5)$$

and choose to put the branch cut of the square root at real $x \in [-1, 1]$. Thus $q^0 \rightarrow i|q_\perp|$ as $|x| \rightarrow \infty$ in any direction. This choice of branch cut ensures that $G^R(q^0(x), q_z(x), q_\perp)$ goes into the standard retarded function as $\text{Im}x \rightarrow 0^+$, and is consistent with the conventions of [18], e.g., this func-

tion has the same analytic structure as the $G^R(x, q_\perp)$ of [18]. Careful inspection of Eq. (A5) then reveals that the imaginary part of q^0 is *positive* for all x , establishing the analyticity in x (for $q^0 = q_z$ and fixed q_\perp). It thus applies to any propagator, extending the claim of [18].

The authors of [18] worked in the Coulomb gauge and found, at intermediate steps, contributions from the large circle at $|x| = \infty$ [proportional to $1/(q_\perp^2 + \frac{1}{3}m_D^2)$], which in the end, precisely canceled out between the longitudinal and transverse channels. These terms did not appear in our calculations, but for a good reason: they are mere gauge artefacts. To see this, we note that the residue at $|x| \rightarrow \infty$ corresponds to a pole at $q^0 = q_z = iq_\perp$, which is an ordinary point in the upper-half q^+ plane: it is thus forbidden by causality. But since a gauge like the Coulomb gauge does not respect causality in a Lorentz-covariant sense (its A^0 field mediates an instantaneous Coulomb interaction), such poles are not forbidden in individual, gauge-dependent terms. They are bound, however, to cancel out in physical quantities like $C(q_\perp)$. Our approach assumes Lorentz-covariant causality from the start and cannot detect such unphysical contributions. A simple solution is to stick to covariant gauges.

-
- [1] K. Adcox *et al.* (PHENIX Collaboration), Phys. Rev. Lett. **88**, 022301 (2001).
 - [2] C. Adler *et al.* (STAR Collaboration), Phys. Rev. Lett. **89**, 202301 (2002).
 - [3] S. A. Bass, C. Gale, A. Majumder, C. Nonaka, G. Y. Qin, T. Renk, and J. Ruppert, Phys. Rev. C **79**, 024901 (2009).
 - [4] P. Arnold and C. Zhai, Phys. Rev. D **51**, 1906 (1995).
 - [5] E. Braaten and A. Nieto, Phys. Rev. Lett. **76**, 1417 (1996).
 - [6] K. Kajantie, M. Laine, K. Rummukainen, and Y. Schroder, Phys. Rev. D **67**, 105008 (2003); F. Di Renzo, M. Laine, V. Miccio, Y. Schroder, and C. Torrero, J. High Energy Phys. **07** (2006) 026.
 - [7] H. Schulz, Nucl. Phys. **B413**, 353 (1994).
 - [8] M. E. Carrington, A. Gynther, and D. Pickering, Phys. Rev. D **78**, 045018 (2008).
 - [9] J. P. Blaizot, E. Iancu, and A. Rebhan, Phys. Rev. D **63**, 065003 (2001).
 - [10] S. Caron-Huot and G. D. Moore, Phys. Rev. Lett. **100**, 052301 (2008); J. High Energy Phys. **02** (2008) 081.
 - [11] M. Laine and Y. Schroder, J. High Energy Phys. **03** (2005) 067.
 - [12] J. P. Blaizot, E. Iancu, and A. Rebhan, Phys. Rev. D **68**, 025011 (2003).
 - [13] K. Kajantie, M. Laine, K. Rummukainen, and Y. Schroder, Phys. Rev. Lett. **86**, 10 (2001).
 - [14] E. Braaten and R. D. Pisarski, Nucl. Phys. **B337**, 569 (1990); J. Frenkel and J. C. Taylor, Nucl. Phys. **B334**, 199 (1990).
 - [15] J. P. Blaizot and E. Iancu, Phys. Rep. **359**, 355 (2002).
 - [16] P. F. Kelly, Q. Liu, C. Lucchesi, and C. Manuel, Phys. Rev. D **50**, 4209 (1994).
 - [17] E. Braaten and M. H. Thoma, Phys. Rev. D **44**, R2625 (1991); **44**, 1298 (1991).
 - [18] P. Aurenche, F. Gelis, and H. Zaraket, J. High Energy Phys. **05** (2002) 043.
 - [19] H. Liu, K. Rajagopal, and U. A. Wiedemann, Phys. Rev. Lett. **97**, 182301 (2006).
 - [20] H. Liu, K. Rajagopal, and Y. Shi, J. High Energy Phys. **08** (2008) 048.
 - [21] J. Casalderrey-Solana and D. Teaney, J. High Energy Phys. **04** (2007) 039.
 - [22] S. S. Gubser, Nucl. Phys. **B790**, 175 (2008).
 - [23] Y. Hatta, E. Iancu, and A. H. Mueller, J. High Energy Phys. **05** (2008) 037.
 - [24] S. S. Gubser, D. R. Gulotta, S. S. Pufu, and F. D. Rocha, J. High Energy Phys. **10** (2008) 052.
 - [25] P. M. Chesler, K. Jensen, A. Karch, and L. G. Yaffe, arXiv:0810.1985.
 - [26] P. Arnold and W. Xiao, Phys. Rev. D **78**, 125008 (2008).
 - [27] G. Y. Qin, J. Ruppert, C. Gale, S. Jeon, G. D. Moore, and M. G. Mustafa, Phys. Rev. Lett. **100**, 072301 (2008).
 - [28] Their description could turn out to be very complicated, though, because jet evolution at $\mathcal{O}(g^2)$ should contain, among other things, the analog of the NLO vacuum DGLAP splitting amplitudes in the presence of the LPM effect (described below). Also, various effects involving

- the scale evolution of the medium constituents and coupling constant evolution should arise.
- [29] R. Baier, Y.L. Dokshitzer, S. Peigne, and D. Schiff, *Phys. Lett. B* **345**, 277 (1995); R. Baier, Y.L. Dokshitzer, A.H. Mueller, S. Peigne, and D. Schiff, *Nucl. Phys.* **B483**, 291 (1997).
- [30] B.G. Zakharov, *JETP Lett.* **65**, 615 (1997); **63**, 952 (1996).
- [31] P. Arnold, G.D. Moore, and L.G. Yaffe, *J. High Energy Phys.* 06 (2002) 030.
- [32] L.D. Landau and I. Pomeranchuk, *Dokl. Akad. Nauk SSSR* **92**, 535 (1953); **92**, 735 (1953); A.B. Migdal, *Dokl. Akad. Nauk SSSR* **105**, 77 (1955); *Phys. Rev.* **103**, 1811 (1956).
- [33] V.N. Gribov and L.N. Lipatov, *Sov. J. Nucl. Phys.* **15**, 438 (1972); **15**, 675 (1972); L.N. Lipatov, *Sov. J. Nucl. Phys.* **20**, 94 (1975); G. Altarelli and G. Parisi, *Nucl. Phys.* **B126**, 298 (1977); Yu.L. Dokshitzer, *Sov. Phys. JETP* **46**, 641 (1977).
- [34] S. Jeon and G.D. Moore, *Phys. Rev. C* **71**, 034901 (2005).
- [35] For instance, one would simply modify $C(q_{\perp})$ in [34], which is actually equal to $C(q_{\perp})/(g^2 C_s T)$ in our conventions.
- [36] I am indebted to G.D. Moore for discussion on this point.
- [37] P. Arnold and C. Dogan, *Phys. Rev. D* **78**, 065008 (2008).
- [38] A. Majumder, arXiv:0810.1367.
- [39] J.I. Kapusta and C. Gale, *Finite temperature field theory: Principles and applications* (Cambridge University Press, Cambridge, UK, 2006), p. 428.
- [40] In strongly coupled theories accessible to gauge-string duality, these two limits are known to be physically distinct. A calculation of \hat{q} for a physical massive quark moving with $v < 1$ (in the sense of its momentum broadening coefficient) by Teaney and Casalderrey-Solana [21], and by Gubser [22], found a divergence $\hat{q} \sim (1 - v^2)^{-1/4} \sqrt{\lambda} T^3$ as $v \nearrow 1$. This calculation is valid for energies $E < M^3/\lambda T^2$, beyond which the coherence time of the force acting on the quark becomes of order the time scale of Langevin dynamics [22]; a time-independent description is then impossible. This suggests that \hat{q} for $v < 1$ should depend on a cutoff time scale, as is the case at weak coupling. On the other hand, the $v \searrow 1$ limit has been studied by Rajagopal, Liu and Wiedemann [19,20], by embedding Euclidean worldsheets into AdS₅ space, and no divergences were met in this limit. It is thus qualitatively quite distinct.
- [41] T. Appelquist and R.D. Pisarski, *Phys. Rev. D* **23**, 2305 (1981).
- [42] K. Farakos, K. Kajantie, K. Rummukainen, and M.E. Shaposhnikov, *Nucl. Phys.* **B425**, 67 (1994).
- [43] Z.T. Liang, X.N. Wang, and J. Zhou, *Phys. Rev. D* **77**, 125010 (2008).
- [44] The dimensionally regulated integrals Eq. (11) have poles in dimensions 2 and 4 but are finite and unambiguous in dimension 3.
- [45] Abelian Wilson loops, computed using Gaussian distribution for gauge fields (as is done by Figs. 3(d)–3(g), for which only the two-point function of the gauge field enters), simply exponentiate: $\langle e^{\int A} \rangle = \exp(\frac{1}{2} \langle \int A \int A \rangle)$. As a consequence, the collision kernel as defined from Eq. (9) is tree-level exact in such theories: there is no interference between scattering events.
- [46] I thank P. Arnold for pointing out a numerical error in an early draft of this paper.
- [47] L.S. Brown, *Phys. Rev. D* **62**, 045026 (2000).
- [48] For high-energy jets (when at least *one* of the energy of the participant is large, $E_{\max} \gg T$), these rotations can be taken to have energy-suppressed angles $\sim q_{\perp}/E$, and thus to have negligible effects on the longitudinal momenta. Even when $E_{\max} \sim T$, the angles are at most $\sim g$ and the changes in longitudinal momenta are $\sim g^2$, beyond the accuracy considered in this paper.
- [49] J. Schwinger, *J. Math. Phys. (N.Y.)* **2**, 407 (1961); L.V. Keldysh, *Sov. Phys. JETP* **20**, 1018 (1964).